

Proton rapidity distribution in nucleus-nucleus collisions at high energy

Fu-Hu Liu

*Institute of Modern Physics and Department of Physics, Shanxi Teachers University
Linfen, Shanxi 041004, China
e-mail: liufh@dns.sxtu.edu.cn*

Recibido el 22 de junio de 2001; aceptado el 4 de octubre de 2001

The proton rapidity distributions in nucleus-nucleus collisions at the Alternating Gradient Synchrotron (AGS) and the Super Proton Synchrotron (SPS) energies are analyzed by the revised thermalized cylinder model. The calculated results are compared and found to be in agreement with the experimental data of Si-Al and Si-Pb collisions at 14.6 AGeV/c, Pb-Pb collisions at 158 AGeV/c, and S-S collisions at 200 AGeV/c.

Keywords: Proton rapidity distribution; nucleus-nucleus collisions; high energy.

La rapidez de distribución de protones en colisiones nucleo-nucleo en las energías de sincrotron de gradiente alternante (AGS) y sincrotron de super proton (SPS) es analizada usando el modelo del cilindro termalizado. Los resultados calculados al ser comparados con los resultados experimentales estan en concordancia con las colisiones de Si-Al y Si-Pb a 14.6 AGeV/c, Pb-Pb a 158 AGeV/c y S-S a 200 AGeV/c.

Descriptores: Rapidez de distribución de protones; colisiones nucleo-nucleo; alta energía.

PACS: 25.75.-q; 25.75.Dw; 24.10.Pa

1. Introduction

Multiparticle production is an important experimental phenomenon in high-energy collisions. A lot of models [1] have been introduced for description of the particle production. Based on the one-dimensional string model [2] and the fireball model [3], we have developed a thermalized cylinder model [4–7] and analyzed the rapidity (or pseudorapidity) distribution of produced particles in high-energy nucleus-nucleus collisions. Considering the contributions of thermalized cylinder and leading particles, the model can give a description of proton rapidity distribution. We notice that the model describes produced particle rapidity distribution and proton rapidity distribution with different considerations. For the produced particle rapidity distribution, only the contribution of thermalized cylinder is considered. For the proton rapidity distribution, both the contributions of thermalized cylinder and leading particles are considered.

In order to describe the produced particle rapidity distribution and the proton rapidity distribution with an unitive consideration, we revise the thermalized cylinder model in this paper. The thermalized cylinder model is introduced shortly, then the revised thermalized cylinder model is given. The calculated results of the revised thermalized cylinder model are compared with experimental data at the Alternating Gradient Synchrotron (AGS) and the Super Proton Synchrotron (SPS) energies. Finally, we give our conclusion.

Let us consider the simplest pictures of the one-dimensional string mode [2] and the fireball model [3]. In a high energy nucleon-nucleon collision, a string is formed consisting of two endpoints acting as energy reservoirs and the interior with constant energy per length. Because of the asymmetry of the mechanism, the string will break into many

substrings along the direction of the incident beam. The distribution length of substrings will define the width of the pseudorapidity distribution. According to the fireball model, the incident nucleon penetrates through the target nucleon, then a firebreak is formed along the direction of the incident beam. The length of the firebreak will define the width of pseudorapidity distribution. In high energy nucleus-nucleus collisions, many strings or firebreaks are formed along the incident direction. Finally, a thermalized cylinder is formed.

According to the thermalized cylinder model, in a given reference frame, we assume that the thermalized cylinder formed in high-energy collisions is in the rapidity range $[y_{\min}, y_{\max}]$. The emission points with the same rapidity, y_x , in the thermalized cylinder form a cross section (emission source) in the rapidity space. For the thermalized cylinder, the initial extensions of the target and projectile are not important because of Lorentz-contraction.

Under the assumption that the particles are emitted isotropically in the rest frame of the emission source, we know that the pseudorapidity (η) distribution of the particles produced in the emission source with rapidity y_x in the concerned reference frame is [4]

$$f(\eta, y_x) = \frac{1}{2 \cosh^2(\eta - y_x)}. \quad (1)$$

If $y_x = y_{\min}$ or y_{\max} , Eq. (1) will describe the η distribution of leading target or projectile particles.

In final state, the η distribution of produced particles (exclusion of the leading particles) is contributed by the whole thermalized cylinder. We have the normalized η distribution of produced particles [4]

$$f(\eta) = \frac{1}{y_{\max} - y_{\min}} \int_{y_{\min}}^{y_{\max}} f(\eta, y_x) dy_x. \quad (2)$$

Considering the contribution of leading particles, we have the normalized η distribution of protons

$$f_p(\eta) = \frac{1 - K_T - K_P}{y_{\max} - y_{\min}} \int_{y_{\min}}^{y_{\max}} f(\eta, y_x) dy_x + K_T f(\eta, y_{\min}) + K_P f(\eta, y_{\max}), \quad (3)$$

where K_T and K_P are the contributions of leading target and projectile particles, and proportional to the target and projectile participant proton numbers, respectively.

For a high-energy particle, if its mass can be neglected comparing with its energy, then the pseudorapidity approximates rapidity (y). The rapidity distribution can be obtained by the above formulas due to $y \approx \eta$ at high energy [8]. Equation (1) describes the pseudorapidity (rapidity) distribution of particles produced in the emission source with rapidity y_x , Eq. (2) gives a description of produced particle pseudorapidity (rapidity) distribution, while Eq. (3) gives a description of proton pseudorapidity (rapidity) distribution.

Let y_C denote the midrapidity of produced particles. We have

$$y_{\min} = y_C - Dy, \quad (4)$$

and

$$y_{\max} = y_C + Dy, \quad (5)$$

where Dy is the rapidity shift in the model. Generally speaking, y_C should be the rapidity of the center-of-mass system of collisions, the peak position of particle rapidity distribution, or the mean value of particle rapidities.

We now revise the thermalized cylinder model. We divide the thermalized cylinder formed in high-energy nucleus-nucleus collisions into two parts: target part and projectile part. In the rapidity space, the target part is in the rapidity range $[y_{T\min}, y_{T\max}]$, and the midrapidity is y_{TC} . While the projectile part is in the rapidity range $[y_{P\min}, y_{P\max}]$, and the midrapidity is y_{PC} . The rapidity of the center-of-mass system of collisions is y_C as that in the thermalized cylinder model. The η distribution of the particles produced in the emission source with rapidity y_x in the concerned reference frame is the same as Eq. (1).

In final state, the η distribution of produced particles or protons is contributed by the target part and the projectile part. According to Eq. (2), we have the normalized η distribution

$$F(\eta) = \frac{K}{y_{T\max} - y_{T\min}} \int_{y_{T\min}}^{y_{T\max}} f(\eta, y_x) dy_x + \frac{1 - K}{y_{P\max} - y_{P\min}} \int_{y_{P\min}}^{y_{P\max}} f(\eta, y_x) dy_x, \quad (6)$$

where K and $1 - K$ are the contributions of target and projectile parts, respectively. For produced particle η distribution, $K = 1/2$. For proton η distribution at a given centrality, $K = N_T/(N_T + N_P)$, where N_T and N_P are the target and projectile participant proton numbers, respectively.

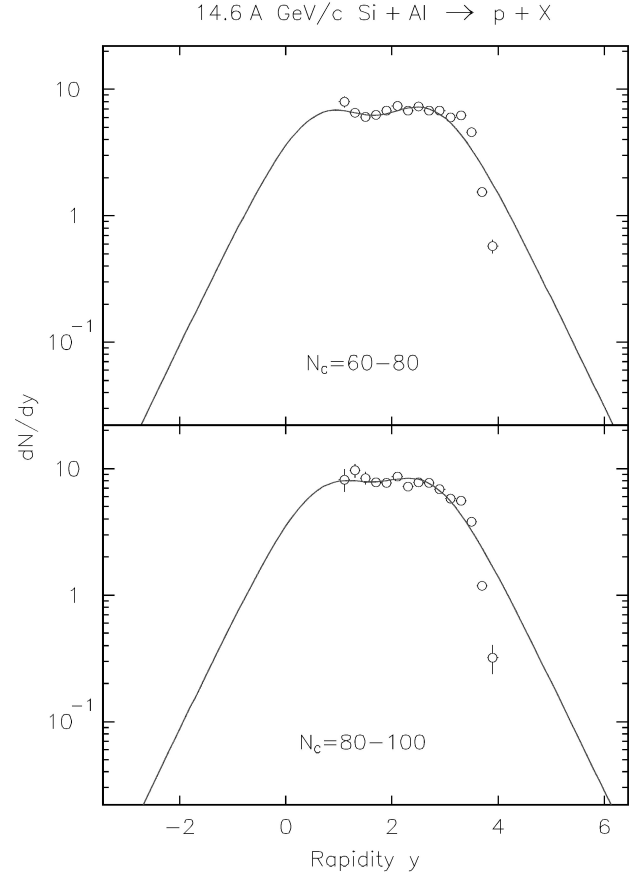


FIGURE 1. Proton rapidity distributions in 14.6 AGeV/c Si+Al \rightarrow p+X collisions for two different charged particle multiplicity regions. Upper figure for $N_C = 60-80$ and lower figure for $N_C = 80-100$. (o) are the experimental data quoted from Ref. 9 and (—) are our calculated results.

Equation (6) is in fact the sum of the contributions of the two cylinders. The target cylinder has a contribution K , while the projectile cylinder has a contribution $1 - K$.

The relationships among $y_C, y_{TC}, y_{PC}, y_{T\min}, y_{T\max}, y_{P\min}$, and $y_{P\max}$ are

$$y_C - y_{TC} = y_{PC} - y_C \equiv \Delta y, \quad (7)$$

and

$$y_{T\max} - y_{TC} = y_{TC} - y_{T\min} = y_{P\max} - y_{PC} = y_{PC} - y_{P\min} \equiv \delta y, \quad (8)$$

where Δy and δy are two rapidity shifts in the revised thermalized cylinder model. Considering Eqs. (7) and (8), Eq. (6) can be rewritten as

$$F(\eta) = \frac{K}{2\delta y} \int_{y_C - \Delta y - \delta y}^{y_C - \Delta y + \delta y} f(\eta, y_x) dy_x + \frac{1 - K}{2\delta y} \int_{y_C + \Delta y - \delta y}^{y_C + \Delta y + \delta y} f(\eta, y_x) dy_x. \quad (9)$$

For produced particle η (or y) distribution, the thermalized cylinder model is the case of $\Delta y = \delta y$ in the revised thermalized cylinder model. In such case, $K = 1/2$,

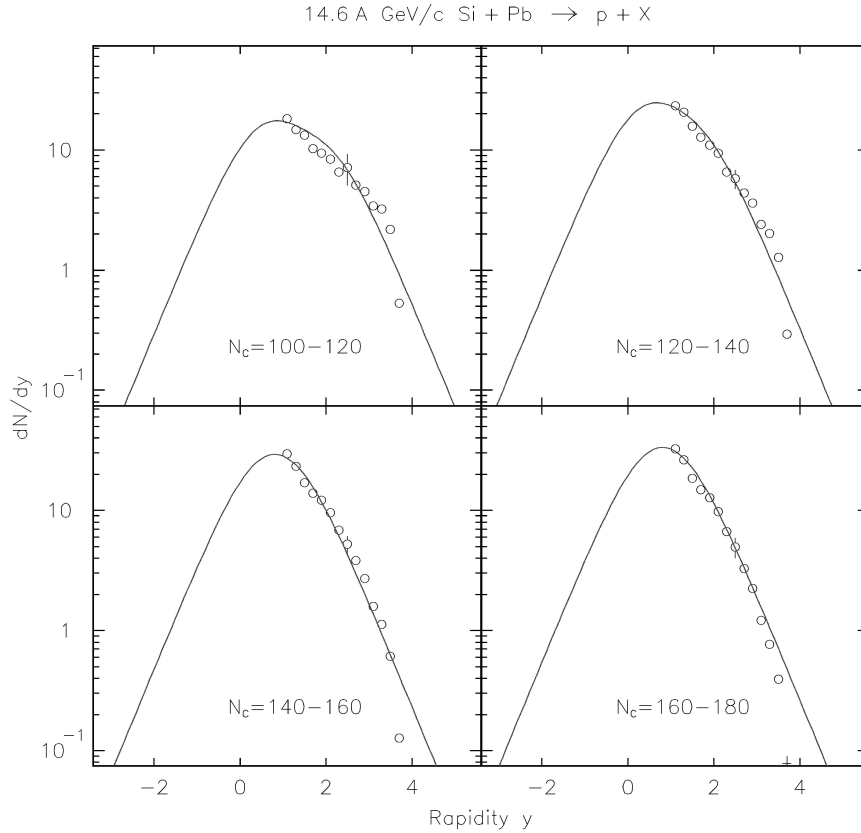


FIGURE 2. Proton rapidity distributions in 14.6 AGeV/c Si+Pb \rightarrow p+X collisions for four different charged particle multiplicity regions. From left to right and up to down $N_C = 100-120$, $N_C = 120-140$, $N_C = 140-160$, and $N_C = 160-180$. (\circ) are the experimental data quoted from Ref. 9 and (—) are our calculated results.

$\Delta y + \delta y = Dy$, $y_{TC} = y_C - Dy/2$, $y_{PC} = y_C + Dy/2$, $y_{Tmin} = y_{min}$, $y_{Tmax} = y_{Pmin} = y_C$, and $y_{Pmax} = y_{max}$. Then, there is no gap between the two cylinders. The two cylinders become one. Equations (6) and (9) become Eq. (2). The revised thermalized cylinder model can replace the thermalized cylinder model. Let $\Delta y = \delta y = Dy/2$, then the η (or y) distribution described by the thermalized cylinder model can be described by the revised thermalized cylinder model.

Figure 1 presents the proton rapidity distributions in 14.6 AGeV/c (AGS energy) Si-Al collisions for two different N_C (multiplicity of charged particles) regions. The circles are the experimental data quoted from Ref. 9. The curves are our calculated results by the revised thermalized cylinder model. In the calculation, $K \approx 13/27 \approx 0.481$. The values of y_C , Δy , and δy for the upper panel are 1.7, 0.9, and 0.2, and for the lower panel are 1.7, 0.8, and 0.2, respectively. The free parameter values are obtained by fitting the experimental data. The values of $\chi^2/\text{degrees of freedom (dof)}$ for the upper and lower panels are 1.21 and 1.25, respectively. One can see that, in the available experimental rapidity region, the calculated results are in agreement with the experimental data except a few data.

Figure 2 presents the proton rapidity distributions in 14.6 AGeV/c (AGS energy) Si-Pb collisions for four

different N_C regions. The circles are the experimental data quoted from Ref. 9. The curves are our calculated results by the revised thermalized cylinder model. The centralities corresponding to different N_C regions from $N_C = 100 - 120$ to $N_C = 160 - 180$ are 16.2%, 8.6%, 2.8%, and 0.5%, respectively [9]. In the calculation, from the centralities 16.2% to 0.5%, $K = 0.675, 0.694, 0.707$, and 0.712 , $y_C = 1.3, 1.0, 0.9$, and 0.9 , $\Delta y = 0.6, 0.5, 0.2$, and 0.2 , and $\delta y = 0.2, 0.2, 0.2$, and 0.2 , respectively. The values of K are obtained by nuclear geometry [10]. Other parameter values are obtained by fitting the experimental data. The values of χ^2/dof for the centralities from 16.2% to 0.5% are 1.09, 1.13, 0.99, and 0.72, respectively. One can see that, in the available experimental rapidity region, the calculated results are in agreement with the experimental data except a few data.

The (net) proton ($p-\bar{p}$) rapidity distribution in central Pb-Pb collisions at 158 AGeV/c (SPS energy) is shown in Fig. 3. The black circles are the experimental data measured by the NA49 Collaboration [11], and the white circles are the data reflected about the midrapidity. The curve is our calculated result by Eq. (9) with $K = 0.5$, $y_C = 2.9$, $\Delta y = 1.3$, and $\delta y = 0.8$. The values of Δy and δy are obtained by fitting the

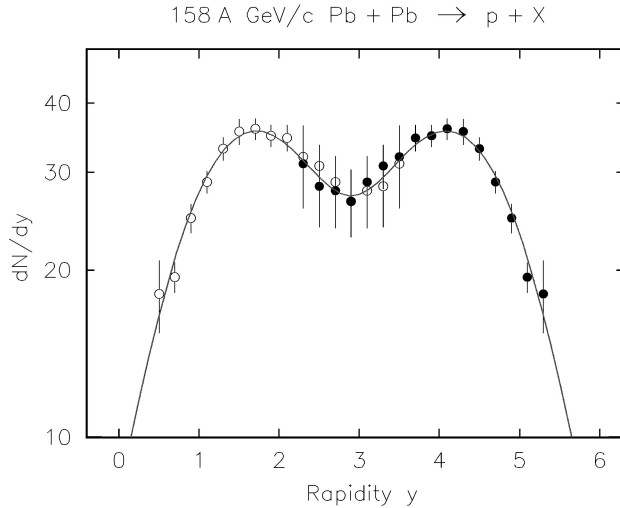


FIGURE 3. Proton rapidity distribution in central Pb+Pb \rightarrow p+X collisions at 158 A GeV/c. (●) are the experimental data measured by the NA49 collaboration [11], (○) are the data reflected about the midrapidity, and (—) is our calculated result.

experimental data. The value of χ^2/dof is 0.68. The Fig. 3 shows that the calculated results are in agreement with the experimental data.

The proton CM (center-of-mass) rapidity distribution in central S-S collisions at 200 A GeV/c (SPS energy) is shown in Fig. 4. The circles are the experimental data measured by the NA35 Collaboration [12]. The curve is our calculated result by Eq. (9) with $K = 0.5$, $y_c = 0.0$, $\Delta y = 1.8$, and $\delta y = 1.4$. The values of Δy and δy are obtained by fitting the experimental data. The value of χ^2/dof is 0.63. The Fig. 4 shows that the calculated results are in agreement with the experimental data.

From the above Figs. (3) and (4) one can see that Eq. (9) can give a description of proton rapidity distribution in nucleus-nucleus collisions at high energy. We know that the thermalized cylinder model is the case of $\Delta y = \delta y$ in the revised thermalized cylinder model for the description of produced particle rapidity distribution. We can say that Eq. (9) gives descriptions of both proton and produced particle rapidity distributions.

The revised version of the thermalized cylinder model is apparently able to describe both the target and projectile

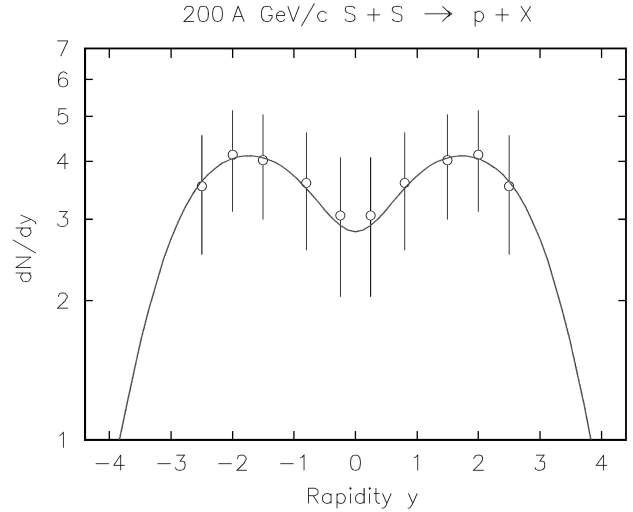


FIGURE 4. Proton CM rapidity distribution in central S+S \rightarrow p+X collisions at 200 A GeV/c. (○) are the experimental data measured by the NA35 collaboration [12] and (—) is our calculated result.

contributions. This renders that both the target and projectile protons are produced in similar fireballs. The target and projectile cylinders are in fact two fireballs extending along the incident beam direction.

To conclude, the revised thermalized cylinder model is successful in the descriptions of rapidity distributions of protons and produced particles in high-energy nucleus-nucleus collisions. Equation (9) describes well the rapidity distributions not only for protons but also for produced particles. The rapidity distributions described by the thermalized cylinder model can be also described by the revised thermalized cylinder model.

Acknowledgements

This work was supported by the China Scholarship Council, Shanxi Provincial Foundation for Returned Overseas Scholars, Shanxi Provincial Foundation for Leading Specialists in Science, and Shanxi Provincial Science Foundation for Young Specialists.

1. J. Geiss, W. Cassing, and C. Greiner, *Nucl. Phys. A* **644** (1998) 107, and references therein.
2. K. Werner, *Phys. Rep.* **232** (1995) 87.
3. W.Y. Chang, *Acta Phys. Sin.* **17** (1961) 271, and references therein; G.D. Westfall *et al.*, *Phys. Rev. Lett.* **37** (1976) 1202.
4. F.H. Liu, *Acta Phys. Sin.* (Overseas Edition) **7** (1998) 321; F.H. Liu, *Chin. J. Phys.* **39** (2001) 243.
5. F.H. Liu and Y.A. Panebratsev, *Nucl. Phys. A* **641** (1998) 379.
6. F.H. Liu and Y.A. Panebratsev, *Phys. Rev. C* **59** (1999) 1798; F.H. Liu and Y.A. Panebratsev, *Phys. Rev. C* **59** (1999) 1193.
7. F.H. Liu, *Nuovo Cimento A* **112** (1999) 1167.
8. "EMU01 Collaboration", M.I. Adamovich *et al.*, *Nucl. Phys. A* **593** (1995) 535.
9. "E814 Collaboration", J. Dee, Ph.D thesis, State University of New York at Stony Brook, USA, (1995).
10. F.H. Liu and Y.A. Panebratsev, *Nuovo Cimento A* **112** (1999) 1143, and references therein.
11. "NA49 Collaboration", H. Appelshäuser *et al.*, *Phys. Rev. Lett.* **82** (1999) 2471; M.Y. Toy, Ph.D. Thesis, University of California at Los Angeles, USA, (1999).
12. "NA35 Collaboration", J. Baechler *et al.*, *Phys. Rev. Lett.* **72** (1994) 1419.